The Physics of Pulsar Scintillation

Ramesh Narayan

Email alerting service   Receive free email alerts when new articles cite this article - sign up in
the box at the top right-hand corner of the article or click **here**

To subscribe to *Phil. Trans. R. Soc. Lond. A* go to:
http://rsta.royalsocietypublishing.org/subscriptions

The physics of pulsar scintillation

By Ramesh Narayan

Harvard-Smithsonian Center for Astrophysics, 60 Garden Street, Cambridge, Massachusetts 02138, U.S.A.

Scintillation is a well-known phenomenon in astronomy, e.g. twinkling of stars due to scattering in the Earth's atmosphere, and variability of compact radio sources due to scattering in the ionosphere and the solar wind. These examples correspond to the so-called régime of weak scattering. Radio pulsars scintillate as a result of scattering in the ionized interstellar medium, but in contrast to the previous cases, the physical régime corresponds to strong scattering. Pulsars exhibit two distinct kinds of variability, called diffractive scintillation and refractive scintillation, on timescales of minutes and weeks respectively. The physics of the various régimes of scintillation are reviewed, and some basic theoretical results are summarized. The properties of imaging in the presence of strong scattering are also discussed.

1. Introduction

When the wavefront from a distant source is perturbed by refractive index fluctuations in an intervening turbulent medium, two effects result at the observer's plane. (i) There are spatial variations in the received flux, which may be observed as temporal scintillation if there are transverse motions of the source, the observer, or the scattering medium. (ii) The image of the source as measured by a telescope is distorted.

The first phenomenon has been known at optical wavelengths since time immemorial. Stars twinkle because of scattering in the Earth's atmosphere. The second phenomenon too has been recognized for a long time. The angular resolution attainable with ground-based optical telescopes is limited by 'atmospheric seeing' to $\approx 1''$. Only recently has this limit been overcome by means of speckle and related interferometric methods on the ground, and by launching telescopes into space.

Investigations of scattering phenomena at radio wavelengths go back almost to the beginning of radio astronomy, with the Cambridge group led by Professor Hewish playing a dominant role. Intensity fluctuations due to the influence of the Earth's ionosphere have been studied since the early 1950s (Smith *et al.* 1950; Hewish 1952; Ratcliffe 1956). More recently, the effect of the ionosphere and the troposphere on images obtained with radio interferometry has attracted wide attention (Hinder & Ryle 1971; Spoelstra & Kelder 1983; Thompson *et al.* 1986). Outside the Earth, the most studied scattering medium is the solar wind, whose turbulence properties have been investigated extensively by using interplanetary scintillation of compact radio sources (Hewish *et al.* 1964; Readhead *et al.* 1978; Hewish 1988). Once the nature of scattering in the solar wind became reasonably well understood, interplanetary scintillation developed into a powerful tool to investigate the angular sizes of distant radio sources (Little & Hewish 1966; Cohen *et al.* 1967).

© 1992 The Royal Society

The phenomena described above generally belong to the régime of 'weak scattering', which is defined in §2 below. Very little attention was devoted in the early days to phenomena associated with the alternate régime of 'strong scattering'. Study of this subject had to await the discovery of radio pulsars and pulsar scintillation. In a landmark paper, Scheuer (1968) explained pulsar variability in terms of interstellar scintillation, and developed the basic concepts of the phenomenon. It is indeed fitting that radio pulsars, whose discovery was an accidental by-product of the Cambridge group's pursuit of radio scintillation, should themselves have opened up a new and fertile branch of astrophysical scattering theory with applications going beyond the field of pulsars.

This article provides a broad introduction to the basic physics of scattering theory, paying particular attention to the régime of strong scattering. The emphasis is on theoretical concepts, leaving the details of observational results to the accompanying article by Professor Hewish. For a more extensive discussion of these topics see the conference proceedings edited by Cordes *et al.* (1988) and the recent review by Rickett (1990). A brief discussion of imaging in the presence of scattering is given in §5.

2. Scattering régimes

To simplify the discussion, assume that the source is at infinity and that the turbulent medium between the source and the observer is replaced by an equivalent thin phase changing screen, the 'scattering screen', at distance D from the observer. (It is straightforward to generalize the theory for a source at a finite distance (Goodman & Narayan 1985). Consideration of an extended medium is less easy, but has been done in several of the studies referred to below, using partial differential or integro-differential equations, and/or a path integral formulation.) If the wavefront from the source has unit amplitude, and if $\varphi(x, y)$ is the phase change introduced by the screen at transverse position (x, y), then the complex wave amplitude immediately after crossing the screen is $\exp[i\varphi(x, y)]$. The amplitude $\psi(X, Y)$ received at position (X, Y) on the observer plane is then given by the Fresnel–Kirchhoff integral (Born & Wolf 1980),

$$\psi(X, Y) = \frac{e^{-i\pi/2}}{2\pi r_F^2} \iint \exp\left[i\varphi(x, y) + i\frac{(x-X)^2 + (y-Y)^2}{2r_F^2}\right] dx\, dy, \qquad (2.1)$$

$$r_F = \sqrt{(\lambda D/2\pi)}, \qquad (2.2)$$

where λ is the wavelength of the radiation, and r_F is the Fresnel scale. (Note, the Fresnel scale is often defined simply as $\sqrt{(\lambda D)}$ without the factor of 2π.) The second term inside the exponential in (2.1) represents the contribution to the phase due to the additional path length from the point (x, y) to (X, Y), under the assumption that $|x-X|, |y-Y| \ll D$, i.e. in the limit of small-angle scattering.

In the absence of any scattering, $\varphi(x, y) = 0$, and (2.1) gives $\psi(X, Y) = 1$. In interpreting this result note that the integrand in (2.1) has unit amplitude and a position-dependent phase, and therefore that the integral is dominated by regions of stationary phase. When $\varphi(x, y) = 0$, the phase is stationary at the point of minimum distance, namely $(x, y) = (X, Y)$, and the integral is dominated by a circular region of radius $\sqrt{2}r_F$ around this point. This patch of the wavefront, the first Fresnel zone, contributes coherently to the integral, while regions outside this zone cancel because of the rapidly oscillating phase.

When there is scattering by a turbulent medium, random phase fluctuations $\varphi(x, y)$ are introduced into the wavefront. In general, these fluctuations will occur on a wide range of scales and their statistics will be described by a power spectrum. Instead of the power spectrum, it is useful to consider the 'phase structure function', $D_\varphi(x, y)$, which represents the mean square phase difference between two points separated by (x, y), i.e.

$$D_\varphi(x, y) = \langle [\varphi(x' + x, y' + y) - \varphi(x', y')]^2 \rangle_{x', y'}. \tag{2.3}$$

In many cases of interest in astronomy, the phase fluctuations arise from Kolmogorov turbulence in the scattering medium. If the turbulence is isotropic and has a sufficiently large outer scale and small inner scale, then the structure function takes the following simple form over the scales of interest,

$$D_\varphi(r) = (r/r_{\text{diff}})^{\frac{5}{3}}, \quad r^2 = x^2 + y^2. \tag{2.4}$$

The normalization of the structure function has been absorbed into the definition of the 'diffractive' length scale r_{diff}, which represents the transverse separation for which the root mean square phase difference is equal to 1 rad. The $\frac{5}{3}$ exponent is characteristic of Kolmogorov turbulence. Note that the structure function of a real scattering medium may differ from (2.4) in several ways, e.g. there may be anisotropy, the exponent may differ from $\frac{5}{3}$, and there may be breaks in the power law behaviour at one or more scales. One of the goals of scintillation theory is to use the observations to deduce the details of the phase structure function, but a discussion of this topic is beyond the scope of this article. (See Narayan (1988) and Rickett (1990) for a discussion of observational constraints on phase fluctuation spectra in the interstellar medium.)

In optical astronomy, it is conventional to use instead of r_{diff} an analogous scale r_0, the 'Fried length', which is defined by

$$D_\varphi(r) = 6.88\,(r/r_0)^{\frac{5}{3}}, \quad r_0 = 3.18 r_{\text{diff}}. \tag{2.5}$$

Apart from a numerical constant, r_{diff} and r_0 represent the same physics, namely the transverse separation over which the phase fluctuation is coherent to within a specified limit (1 rad and $\sqrt{6.88}$ rad respectively).

Having introduced the two basic lengthscales r_F and r_{diff}, we are now in a position to define the régimes of weak and strong scattering.

Weak scattering. This is the régime where $r_{\text{diff}} \gg r_F$, so that, by (2.4), $D_\varphi(r_F) \ll 1$. The latter condition implies that the random phase fluctuations within the first Fresnel zone are small. Because of this, the basic concept of the Fresnel zone survives, and there are only weak perturbations in the wavefront that arrives at the observer plane. The nature of the scintillations in this régime of scattering is summarized in §3.

Strong scattering. Here $r_{\text{diff}} \ll r_F$, which implies that $D_\varphi(r_F) \gg 1$. Since the random phase fluctuations due to the scattering screen vary by many radians over the Fresnel scale, the length scale r_F loses its relevance. Instead, r_{diff} takes over as the characteristic size of a coherent patch, since it is the scale on which the phase may be considered to be approximately constant (to within a radian). Moreover, for each point (X, Y) on the observer plane, there will be many points (x, y) on the scattering screen with stationary phase, leading to 'multipath propagation'. These ideas are discussed further in §4.

Table 1. *Examples of scattering media in astronomy, with typical values of* λ, D, r_{F}, *and* r_{diff}

medium	$\dfrac{\lambda}{\mathrm{cm}}$	$\dfrac{D}{\mathrm{cm}}$	$\dfrac{r_{\mathrm{F}}}{\mathrm{cm}}$	$\dfrac{r_{\mathrm{diff}}}{\mathrm{cm}}$	régime of scattering	
					weak	strong
optical						
Earth's atmosphere	5×10^{-5}	10^6	3	10	mostly	near horizon
planetary atmospheres[a]	10^{-4}	10^{14}	4×10^4	$10^2 - 10^6$	early in occultation	deep in occultation
radio						
troposphere	20	10^5	6×10^2	$\sim 10^5$	yes	no
ionosphere	3×10^2	3×10^7	4×10^4	$\sim 10^5$	yes	sometimes
solar wind	10^2	10^{13}	10^7	$> 10^7$	mostly	close to the Sun
interstellar medium	10^2	10^{21}	10^{11}	$\sim 10^9$	no	yes

[a] Stars scintillate due to scattering in planetary atmospheres during occultations. The scattering is initially weak but becomes strong deep in the occultation (cf. Narayan & Hubbard 1988).

Table 1 lists typical parameters for a number of scattering media in astronomy where scintillation and image distortions are known to take place. The nature of the scattering régime, whether weak or strong, is indicated. For ionospheric, inter-planetary, and interstellar scattering, all of which involve ionized media, the cold plasma dispersion relation can be combined with the Kolmogorov turbulence spectrum to show that

$$r_{\mathrm{diff}} \propto \lambda^{-\frac{6}{5}} D^{-\frac{3}{5}}, \quad r_{\mathrm{diff}}/r_{\mathrm{F}} \propto \lambda^{-\frac{17}{10}} D^{-\frac{11}{10}}, \tag{2.6}$$

where D represents the pathlength through the turbulent medium. The strength of scattering thus increases with increasing wavelength and distance. Note from table 1 that interstellar radio scintillation corresponds to strong scattering over most of the range of wavelengths and distances of interest for pulsar observations.

3. Scintillation in weak scattering $(r_{\mathrm{diff}} \gg r_{\mathrm{F}})$

The flux of radiation received at position (X, Y) on the observer plane from a point source is described by the quantity

$$F(X, Y) = |\psi(X, Y)|^2. \tag{3.1}$$

In weak scattering, $\psi(X, Y)$ has weak perturbations around its unscattered value of unity, leading to small variations in the measured flux. The dominant influence on the flux is due to the mild focusing/defocusing action of phase fluctuations with length scales $\approx r_{\mathrm{F}}$. For an observer whose first Fresnel zone coincides with a focusing segment of phase fluctuation, the size of the coherent patch becomes greater than r_{F} because the phase variation due to the geometrical term $(\boldsymbol{r} - \boldsymbol{R})^2 / 2r_{\mathrm{F}}^2$ in (2.1) is partly offset by the counter variation of $\varphi(x, y)$. Consequently, $F(X, Y) > 1$ for such an observer. Similarly, $F(X, Y) < 1$ for an observer who is aligned with a defocusing region of the phase screen. Further, because of the dominant role played by the Fresnel scale, the Fresnel–Kirchhoff propagator in (2.1) behaves effectively like a low-pass spatial filter with length scale r_{F}. Consequently, the flux scintillation is expected to be primarily on this scale.

Since the flux variations are stochastic in nature, it is most useful to consider its statistical properties. Define the power spectrum of $F(X, Y)$ to be $\tilde{W}_{\mathrm{p}}(q)\,\mathrm{d}^2q$, where q is a spatial wavevector and the subscript 'p' indicates that the result refers to a point

source. A more useful quantity is the fluctuation power per logarithmic interval of q, namely, $q^2 \tilde{W}_p(q)$, since it represents the mean square variations in the flux on the lengthscale $1/q$. For the structure function given in (2.4), this takes the form (Matheson & Little 1971; Uscinski 1977; Tatarskii & Zavorotnyi 1980)

$$q^2 \tilde{W}_p(q) = C(r_F/r_{diff})^{\frac{5}{3}} ((qr_F)^{-\frac{5}{3}} \sin^2 (\tfrac{1}{2} q^2 r_F^2)), \tag{3.2}$$

where $C (= 11.2)$ is a numerical constant. For wavevectors $q < 1/r_F$, i.e. length scales longer than r_F, the power increases with increasing q as $q^{\frac{7}{3}}$, while for $q > 1/r_F$ the power decreases as $q^{-\frac{5}{3}}$. Thus the flux variations are strongest at the Fresnel scale, as expected from the physical argument given in the previous paragraph. If there is a transverse velocity v between the scattering medium and the observer-source line-of-sight, then temporal scintillations will be observed with a timescale t_{scint} given by the Fresnel timescale,

$$t_F = r_F/v. \tag{3.3}$$

Note that the lengthscale and the timescale are independent of the strength of scattering.

By (3.2), 'the modulation index', i.e. the root mean square amplitude of the flux scintillation, is $m_p \approx (r_F/r_{diff})^{\frac{5}{6}} < 1$, which implies that the flux variations are weak. This is the origin of the terms 'weak scattering' and 'weak scintillation' associated with this régime. The scaling of the modulation index is easy to understand. The root mean square (r.m.s.) flux variations should be of the order of $D/f(r_F)$, where $f(r_F)$ is the r.m.s. focal length of phase fluctuations on the scale r_F, given approximately by $f(r_F) \approx r_F^2/\lambda D_\phi^{\frac{1}{2}}(r_F)$. The modulation index is therefore $m_p \approx (r_F/r_{diff})^{\frac{5}{6}}$. Note that $f(r_F)$ becomes of order D, and the modulation index becomes of order unity, when $r_{diff} = r_F$. This represents the transition from weak to strong scattering. For $r_{diff} < r_F$ there is overfocusing and we enter the régime of strong scattering whose properties are discussed in §4.

Two further points to note in weak scattering are the following. First, the intensity variations are correlated over a wide bandwidth, so that the 'decorrelation bandwidth' $\Delta \nu_{dc}$ is of the order of the frequency ν (or, equivalently, $\Delta\lambda \approx \lambda$). Second, although the result (3.2) is strictly true only for a point source, the fluctuations are essentially the same for a finite source so long as the angular size θ_S of the source is smaller than the Fresnel angle, defined by

$$\theta_F = r_F/D. \tag{3.4}$$

Collecting all the results, weak scintillation of a point source satisfies the following scalings:

$$\text{weak scattering – point source } (\theta_S < \theta_F)$$

$$\left.\begin{aligned} r_{scint} &\approx r_F, & t_{scint} &\approx t_F = r_F/v, \\ m_p &\approx (r_F/r_{diff})^{\frac{5}{6}} < 1, & \delta\nu_{dc} &\approx \Delta\nu_{dc}/\nu \sim 1. \end{aligned}\right\} \tag{3.5}$$

The scalings are illustrated in figure 1.

In the case of an extended (incoherent) source, the net scintillation pattern on the observer plane is the sum of the flux variations due to all the elements in the source. The intensity patterns due to two source elements separated by an angle $\boldsymbol{\theta}$ are identical except that they are shifted on the observer plane by a linear offset $-D\boldsymbol{\theta}$. Suppose for simplicity that the source has a gaussian intensity profile of the form

$$I_S(\boldsymbol{\theta}) = (1/\pi\theta_S^2) \exp[-|\boldsymbol{\theta}|^2/\theta_S^2]. \tag{3.6}$$
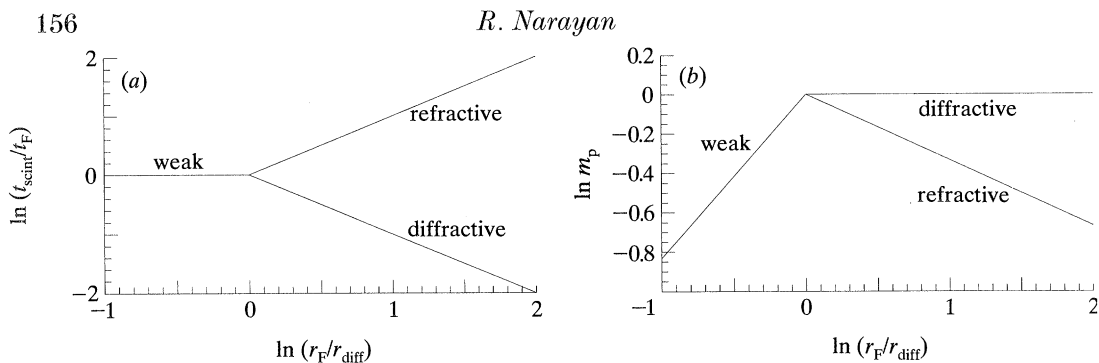
Figure 1. (*a*) The timescale of scintillation along the vertical axis as a function of the scattering strength along the horizontal axis. Weak scattering is to the left of the diagram ($r_{diff} > r_F$), and strong scattering is to the right ($r_{diff} < r_F$). In weak scattering, the scintillation occurs with a single characteristic timescale, the Fresnel timescale t_F defined in (3.3), while in strong scattering, there are two kinds of variability, diffractive and refractive scintillation, with distinct timescales. (*b*) The variation of the flux modulation index m_p as a function of scattering strength. The lines represent asymptotic results and are not reliable in the transition region where $r_{diff} \approx r_F$.

The power spectrum of the flux variations is then given by

$$\tilde{W}_e(q) = \tilde{W}_p(q) \exp[-\tfrac{1}{2}q^2 D^2 \theta_S^2], \tag{3.7}$$

where the subscript 'e' refers to an extended source. In this case, the flux variations cut off at a wave vector $q \approx 1/D\theta_S$ (rather than at $q \approx 1/r_F$ as in the point source case). This is because, in effect, the source acts like a spatial filter of linear size $D\theta_S$. Consequently, the scintillation timescale is given by $D\theta_S/v$. Further, since the power spectrum $q^2\tilde{W}(q)$ varies as $q^{\frac{7}{3}}$ for $q < 1/r_F$, the mean square intensity fluctuations are suppressed relative to the case of a point source by a factor of $(\theta_F/\theta_S)^{\frac{7}{3}}$, i.e. the modulation index is suppressed by $(\theta_F/\theta_S)^{\frac{7}{6}}$. Summarizing these properties, scintillation of an extended source in the presence of weak scattering has the following characteristics:

weak scattering – extended source ($\theta_S > \theta_F$)

$$\left. \begin{array}{ll} r_{scint} \approx \theta_S D = r_F(\theta_S/\theta_F), & t_{scint} \approx t_F(\theta_S/\theta_F), \\ m_e \approx (r_F/r_{diff})^{\frac{5}{6}}(\theta_F/\theta_S)^{\frac{7}{6}} < m_p < 1, & \delta\nu_{dc} \approx 1. \end{array} \right\} \tag{3.8}$$

For scattering of optical radiation in the Earth's atmosphere, stars correspond to the point source limit given in (3.5), while planets, because of their larger angular sizes, correspond to (3.8). Therefore, planets have much weaker scintillation than stars, and their flux variations, if any, must occur on slower timescales than observed in stellar twinkling. The same principle has been used to set limits on the angular diameters of extragalactic radio sources by observing the amplitude and timescale of their interplanetary scintillation (Little & Hewish 1966; Cohen *et al.* 1967).

The parameters listed in table 1 indicate that a number of examples of scattering in astronomy belong to the weak scattering régime. In some cases such as radio scattering in the troposphere, r_F/r_{diff} is so small that amplitude scintillation is virtually never observed. In many of the other cases, $r_F/r_{diff} \approx$ a few percent to a few tens of percent, and so there are measurable levels of intensity variations (e.g. twinkling of stars, interplanetary scintillation of compact radio sources). In several examples, the ratio r_F/r_{diff} varies strongly as a function of some parameter of the observations and crosses over into the strong scattering régime under certain circumstances. This happens for the twinkling of stars for lines of sight close to the

horizon, for scintillations deep inside planetary occultations, for interplanetary scintillation close to the sun and at long wavelengths, and for ionospheric scintillation at very long wavelengths.

4. Scintillation in strong scattering ($r_{\text{diff}} \ll r_{\text{F}}$)

The spectrum of flux variations $\widetilde{W}_{\text{p}}(q)$ due to a point source in the régime of strong scattering was originally calculated by Gochelashvily & Shishov (1975) (see also Rumsey 1975; Prokhorov *et al.* 1975; Tatarskii & Zavorotnyi 1980; Uscinski 1982; Goodman & Narayan 1985), and is given by

$$\left.\begin{aligned} q^2 \widetilde{W}_{\text{p}}(q) &= C(r_{\text{F}}/r_{\text{diff}})^{\frac{5}{3}}(qr_{\text{F}})^{\frac{7}{3}}\exp\left[-(qr_{\text{ref}})^{\frac{5}{3}}\right], \quad q \lesssim r_{\text{ref}}^{-1}, \\ &= C'(qr_{\text{diff}})^2, \quad r_{\text{ref}}^{-1} \lesssim q < r_{\text{diff}}^{-1}, \\ &= C''(qr_{\text{diff}})^{-\frac{5}{3}}, \quad r_{\text{diff}}^{-1} < q, \end{aligned}\right\} \tag{4.1}$$

where C, C' and C'' are numerical constants. Equation (4.1) involves a new length scale, the 'refractive lengthscale' r_{ref}, which is defined by

$$r_{\text{ref}} = r_{\text{F}}^2/r_{\text{diff}} \gg r_{\text{diff}}. \tag{4.2}$$

The most important feature to notice in (4.1) is that the spectrum has two peaks at widely separated length scales. The dominant peak occurs at $qr_{\text{diff}} \approx 1$, corresponding to flux variations on lengthscales $\approx r_{\text{diff}}$. This branch is referred to as 'diffractive scintillation' and its physics was explained by Scheuer (1968). The second peak at $qr_{\text{ref}} \approx 1$ corresponds to relatively weak scintillation on the much longer refractive scale r_{ref}, and is referred to as 'refractive scintillation'. Although the existence of the second branch of scintillation was known since 1974, its relevance to astrophysics was recognized only after the pathbreaking work of Sieber (1982) and Rickett *et al.* (1984). The physics of the two kinds of scintillation is discussed below.

(a) Diffraction scintillation

As described in §2, a key feature of the strong scattering régime is multipath propagation, whereby each point on the observer plane receives radiation from a large number of points on the scattering screen. To visualize the situation, imagine the scattering screen to be sub-divided into a number of coherent patches surrounding the points of stationary phase (Goodman *et al.* 1987). Each patch has a size $\approx r_{\text{diff}}$, and the patches are randomly distributed with separations $\approx r_{\text{diff}}$. Each coherent patch scatters radiation into a diffraction cone of angle

$$\theta_{\text{scatt}} \sim \lambda/r_{\text{diff}} \sim r_{\text{ref}}/D. \tag{4.3}$$

Therefore, a given observer is illuminated by all patches that lie within a region of size $\approx D\theta_{\text{scatt}} \approx r_{\text{ref}}$ on the scattering screen. Since the observer receives rays covering a range of angles $\approx \theta_{\text{scatt}}$, the image of a point source will appear to be 'scatter-broadened' by this angle. Further, (4.3) shows that the refractive length scale r_{ref}, defined in (4.2), corresponds to the size of the scatter-broadened image projected back on the scattering screen ($r_{\text{ref}} = D\theta_{\text{scatt}}$).

The number of rays contributing to a given point on the observer plane is very large, $\approx (r_{\text{ref}}/r_{\text{diff}})^2 = (r_{\text{F}}/r_{\text{diff}})^4$, and each ray has a random phase that is essentially uncorrelated with the phases of its neighbours. The various rays will therefore interfere with one another to give a random interference pattern. (The famous Young's slits experiment is helpful to visualize the interference pattern associated

with diffractive scintillation.) Since the rays span a range of angles $\approx \theta_{\text{scatt}}$, therefore the characteristic length scale of the flux variations is $\approx \lambda/\theta_{\text{scatt}} \approx r_{\text{diff}}$. This corresponds to the peak at $qr_{\text{diff}} \approx 1$ in the power spectrum of (4.1). Further, it is easy to see that the flux variations $F(X, Y)$ will satisfy Rayleigh statistics (two-dimensional random walk in the complex plane), with saturated fluctuations, i.e.

$$\langle F \rangle = 1, \quad \langle (F - \langle F \rangle)^2 \rangle = 1. \tag{4.4}$$

This means that the modulation index m_{p} will be equal to unity, as confirmed by (4.1). The scintillation timescale is given by

$$t_{\text{diff}} = r_{\text{diff}}/v. \tag{4.5}$$

Since the scintillation lengthscale is r_{diff}, the critical angular scale that distinguishes point sources from extended sources is

$$\theta_{\text{diff}} = r_{\text{diff}}/D = (r_{\text{diff}}/r_{\text{F}})^2 \theta_{\text{scatt}} \ll \theta_{\text{scatt}}. \tag{4.6}$$

The nature of the scintillations of an extended source can be calculated from (4.1) by using arguments similar to those presented in §3. In particular, a gaussian source introduces a spatial low-pass filter as in (3.7), leading to an increase in the scintillation timescale and a reduction of the modulation index. Diffractive scintillation is a narrow-band phenomenon, the fractional decorrelation bandwidth being given by $\delta\nu_{\text{dc}} \approx (r_{\text{diff}}/r_{\text{F}})^2$. (The Young's experiment analogy is helpful to see this.) Collecting together all the results, we thus have the following scalings for diffractive scintillation of point and extended sources (see figure 1):

diffractive strong scintillation – point source ($\theta_{\text{S}} < \theta_{\text{diff}}$)

$$\left.\begin{aligned} r_{\text{scint}} &\approx r_{\text{diff}}, \quad t_{\text{scint}} \approx t_{\text{diff}} = r_{\text{diff}}/v, \\ m_{\text{p}} &\approx 1, \quad \delta\nu_{\text{dc}} \approx (r_{\text{diff}}/r_{\text{F}})^2 \ll 1. \end{aligned}\right\} \tag{4.7}$$

diffractive strong scintillation – extended source ($\theta_{\text{S}} > \theta_{\text{diff}}$)

$$\left.\begin{aligned} r_{\text{scint}} &\approx D\theta_{\text{S}} \approx r_{\text{diff}}(\theta_{\text{S}}/\theta_{\text{diff}}), \quad t_{\text{scint}} \approx t_{\text{diff}}(\theta_{\text{S}}/\theta_{\text{diff}}), \\ m_{\text{e}} &\approx \theta_{\text{diff}}/\theta_{\text{S}} < 1, \quad \delta\nu_{\text{dc}} \approx (r_{\text{diff}}/r_{\text{F}})^2 \ll 1. \end{aligned}\right\} \tag{4.8}$$

Diffractive scintillation due to scattering in the interstellar medium was detected in radio pulsars from the earliest days. For a canonical pulsar velocity of $v \approx 10^7$ cm s^{-1} and $r_{\text{diff}} \approx 10^9$ cm, the variability timescale is $t_{\text{diff}} \approx 10^2$ s. Diffractive scintillation is present in all pulsars at all wavelengths and has been much investigated because of the wealth of information it provides on density fluctuations in the interstellar medium as well as on the transverse velocities of pulsars (Cordes *et al.* 1988; Rickett 1990). This topic is discussed in greater detail in the accompanying article by Professor Hewish. Because of the very strict limit on the angular size of the source, virtually no radio source other than pulsars (except possibly some masers) is known to show diffractive scintillation.

(b) Refractive scintillation

The second kind of scintillation in the régime of strong scattering is called refractive scintillation. This occurs as a result of large-scale inhomogeneities in the scattering screen on length scales $\approx r_{\text{ref}}$, the size of the projected scatter-broadened image. The intensity fluctuations on the observer plane also have a correlation length $\approx r_{\text{ref}}$, leading to a scintillation timescale

$$t_{\text{ref}} = r_{\text{ref}}/v. \tag{4.9}$$

Refractive flux variations cause the secondary bump at $qr_{ref} \approx 1$ in the power spectrum given in (4.1).

Refractive scintillation can be understood almost entirely in terms of geometrical optics (Blandford & Narayan 1985; Romani *et al.* 1986). Consider a phase fluctuation of linear size $\approx r_{ref}$ located on the scattering screen in such a way as to focus radiation towards the observer. This phase profile will tilt towards its focus all the diffraction cones of the individual r_{diff}-sized coherent patches discussed in §4*a*. Consequently, the observer will receive radiation from a larger number of coherent patches and therefore will see a larger flux. The reverse is the case if the phase fluctuation has a defocusing profile. The amplitude of the flux variations depends on the r.m.s. focal length of phase fluctuations with scales $\approx r_{ref}$, given approximately by

$$f(r_{ref}) \approx r_{ref}^2/\lambda D_{\varphi}^{\frac{1}{2}}(r_{ref}) \approx D(r_F/r_{diff})^{\frac{1}{3}}.$$

Since $f(r_{ref}) \gg D$, the flux variations are weak, the modulation index being given by $m_p \approx D/f(r_{ref}) \approx (r_{diff}/r_F)^{\frac{1}{3}}$.

In contrast to diffractive scintillation, refractive scintillation is broadband in nature with $\delta\nu_{dc} \approx 1$. Also, it has a much less severe limit on the angular size of the source; the source merely has to be smaller than $\theta_{scatt} = r_{ref}/D$. If the source is larger than this limit, the scintillation timescale becomes longer and the modulation index smaller, exactly as in the previous cases.

Summarizing the basic characteristics of refractive scintillation we have the following results (see figure 1):

refractive strong scattering – point source $(\theta_S < \theta_{scatt})$

$$\left.\begin{array}{ll} r_{scint} \approx r_{ref} \gg r_{diff}, & t_{scint} \approx t_{ref} \gg t_{diff}, \\ m_p \approx (r_{diff}/r_F)^{\frac{1}{3}} < 1, & \delta\nu_{dc} \approx 1. \end{array}\right\} \qquad (4.10)$$

refractive strong scattering – extended source $(\theta_S > \theta_{scatt})$

$$\left.\begin{array}{ll} r_{scint} \approx D\theta_S \sim r_{ref}(\theta_S/\theta_{scatt}), & t_{scint} \approx t_{ref}(\theta_S/\theta_{scatt}), \\ m_e \approx (r_{diff}/r_F)^{\frac{1}{3}}(\theta_{scatt}/\theta_S)^{\frac{7}{6}} < m_p < 1, & \delta\nu_{dc} \approx 1. \end{array}\right\} \qquad (4.11)$$

Pulsar variability due to refractive scintillation was detected already in 1970 by Cole *et al.* (1970), but for a decade it was assumed that the variations were intrinsic to the source. The breakthrough came when Sieber (1982) noticed that the variability timescale is correlated with the distance to the pulsar and remarked that this must imply that the flux variations are caused by a propagation effect. The actual physical explanation was provided by Rickett *et al.* (1984) who drew on earlier theoretical work by Shishov (1974) and Gochelashvily & Shishov (1975). For a typical pulsar, $v \approx 10^7$ cm s^{-1} and $r_{ref} \approx 10^{13}$ cm, and so the variability timescale is $t_{ref} \approx 10^6$ s $\approx$ weeks.

Because refractive scintillation imposes relatively modest limits on the source size and the bandwidth (equation (4.11)), the phenomenon is not exclusive to pulsars (as diffractive scintillation is); it is seen also in other compact radio sources such as masers and extragalactic radio sources. Indeed, the recognition of refractive scintillation solved the longstanding problem of 'low frequency variability' of radio galaxies (Shapirovskaya 1978; Rickett *et al.* 1984; Blandford *et al.* 1986; Rickett 1986). For long this variability was interpreted as being intrinsic to the source, but this led to severe theoretical difficulties in many instances since it implied extremely small source sizes and unphysically large energy densities. If the same variability is reinterpreted as a propagation effect, then the requirements on the source are much

more reasonable. It is currently believed that much (though not all) of the variability observed in extragalactic radio sources at frequencies $\lesssim 1$ GHz is due to refractive scintillation.

While diffractive and refractive scintillation are usually quite distinct, under certain circumstances the differences between the two can be blurred. If the spectrum of phase fluctuations has an inner scale r_{in} larger than r_{diff}, then certain new phenomena can arise because of the effect of caustics (Goodman *et al.* 1987). The physics can be understood by slightly modifying the picture of multipath propagation described in §4*a*. It is still correct to think of coherent patches with sizes $\approx r_{diff}$ (in practice, this is how r_{diff} is defined, e.g. equation (2.4)). However, the different coherent patches on the scattering screen are now separated by distances $\approx r_{in}$ rather than r_{diff}. Caustics then arise whenever two (or more) neighbouring patches approach each other as a function of time, brightening in the process. The observed flux variation has an envelope which can be understood purely in terms of ray optics (which makes it a refractive effect); however, over and above this slow variation, there will also be rapid variations due to interference between the multiple rays contributing to the caustic (giving the phenomenon a diffractive aspect as well). Berry & Upstill (1980) review the morphologies of caustics and their diffraction patterns.

When there are caustics in the observed scintillation, the flux modulation index will increase relative to the case without caustics ($r_{in} < r_{diff}$). There have been some claims that pulsars and compact extragalactic radio sources do have somewhat excessive flux variations. Motivated by this, Coles *et al.* (1987) proposed that the inner scale of turbulence in the interstellar medium may be as large as $\approx 10^{11}$ cm, much larger than the diffractive scale ($r_{diff} \approx 10^8$–10^9 cm). However, Kaspi & Stinebring (1992) conclude on the basis of careful long-term monitoring of a number of pulsars that the observed modulation indices are inconsistent with such large values of r_{in}. In fact, their observations are consistent with a Kolmogorov spectrum with $r_{in} < r_{diff}$.

Caustic-like events on a scale $\approx 10^{14}$ cm, rather than 10^{11} cm, may have been seen directly in the so-called 'extreme scattering events' discovered by Fiedler *et al.* (1987). These events involve the sudden brightening and dimming of extragalactic radio sources, with a particular double-peaked time profile. Romani *et al.* (1987) suggested that Fiedler *et al.* had observed caustic events produced by clouds of ionized gas with electron number densities ≈ 100 cm^{-3} and linear sizes $\approx 10^{14}$ cm. Extreme scattering events are not common, implying that the associated electron clouds are quite rare in the Galaxy.

5. Scattering and imaging

The effect of weak scattering on images has been extensively studied, particularly with reference to optical imaging through the Earth's atmosphere. The nature of the image obtained with a telescope is known to depend critically on the integration time t_{int} over which the image is averaged. If $t_{int} \gg t_{diff} = r_{diff}/v$, then the random phase fluctuations due to the scattering medium degrade the resolution of the image to the angular size of the seeing disc, which is $\approx \theta_{scatt} = \lambda/r_{diff}$. For such long integrations, even if the telescope has an aperture larger than r_{diff}, the resolution is still limited to θ_{scatt}.

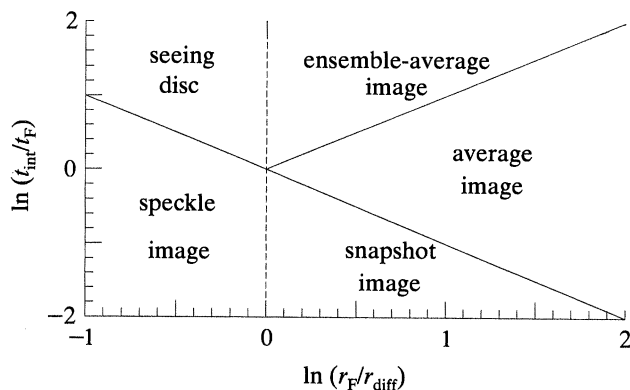On the other hand, if $t_{int} < t_{diff}$, then the distortions due to the phase fluctuations

Figure 2. The various régimes of imaging, indicated as a function of the integration time plotted along the vertical axis and the strength of scattering shown along the horizontal axis. In weak scattering ($r_{diff} > r_F$), there are two régimes of imaging, corresponding to long integration times (seeing disc) and short integration times (speckle image). In strong scattering ($r_{diff} < r_F$), there are two characteristic timescales in the scintillation, and correspondingly there are three régimes of imaging (ensemble-average image, average image, and snapshot image).

are frozen in for the duration of the observations. In this limit, it turns out that a single aperture telescope produces an image consisting of several 'speckles' (provided the bandwidth is sufficiently small) with individual sizes $\approx \lambda/a$, where a is the diameter of the aperture (Roddier 1981; Dainty 1984). By analysing the shapes of the speckles one can study the source with angular resolution equivalent to that of the full telescope aperture. The signal-to-noise ratio will not be as good as that possible with an undistorted wavefront because the energy from the source is distributed over several independent speckles. Also, of course, the need to limit t_{int} below the diffractive timescale, and the bandwidth below a critical value, reduces the sensitivity of the observations. Nevertheless, impressive results have been obtained on a number of astronomical objects, particularly in the infrared (Gorham *et al.* 1989; Ghez *et al.* 1991).

The situation is a little better when one is doing aperture synthesis with an interferometer. Using a powerful technique called self-calibration, the phase and amplitude errors at the individual elements of the interferometer can be eliminated (Jennison 1958; Readhead & Wilkinson 1978; Cornwell & Wilkinson 1981; Pearson & Readhead 1984). This permits reconstruction of the true undistorted image corresponding to the unscattered wavefront. Self-calibration has found extensive application in radio interferometry for correcting the effects of the Earth's troposphere and ionosphere. Some preliminary work at optical wavelengths indicates great promise in this area as well (Haniff *et al.* 1987).

The nature of imaging in the presence of strong scattering has been investigated only recently (Narayan & Goodman 1989; Goodman & Narayan 1989; Cornwell *et al.* 1989; Narayan *et al.* 1989, 1990), and turns out to be quite fascinating. The key point is that the multipath propagation automatically introduces two very distinct timescales into the problem, namely t_{diff} and t_{ref}. Correspondingly, there are three régimes of imaging (figure 2), which have been assigned the following names: ensemble-average image ($t_{int} > r_{ref}$), average image ($t_{ref} > t_{int} > t_{diff}$), snapshot image ($t_{diff} > t_{int}$). (The definitions of the régimes also involve constraints on the bandwidth which we do not discuss here.) Each of the three régimes of imaging has distinct properties, as discussed in the above papers.

The ensemble-average and average image régimes are easiest to access, and have already been used to study the nature of density fluctuations in the interstellar medium (Gwinn *et al.* 1988; Mutel & Lestrade 1990). Moreover, preliminary imaging experiments with compact radio sources whose lines-of-sight go very close the Sun have been successful in probing the region of the solar wind close to the Sun where, as indicated in table 1, the parameters correspond to the strong scattering régime (Narayan *et al.* 1989). Indeed, by combining such imaging observations of radio pulsars with simultaneous monitoring of variations in dispersion measure and rotation measure (which probe fluctuations in the integrated electron density and line-of-sight magnetic field), it will be possible to obtain quite a detailed picture of the hydrodynamics and magnetic field configuration of the solar wind in the acceleration zone (Hankins *et al.* 1989). A few bright pulsars, including the Crab pulsar, are sufficiently close to the ecliptic plane to permit such a study.

The third régime of imaging, the snapshot régime, has perhaps the most interesting properties. Cornwell *et al.* and Narayan *et al.* (1990) have argued that, in principle, one could use a snapshot image measured with a suitably designed interferometer to image the source with an angular resolution given by $\theta_{\mathrm{diff}} = r_{\mathrm{diff}}/D \approx \lambda/r_{\mathrm{ref}}$. In other words, one can map the source with a resolution equivalent to that of a telescope of aperture equal to r_{ref} even though the actual telescope may have a much smaller aperture. This possibility has not yet been demonstrated in practice, but some preliminary tests using scattering in the solar wind have been successful (Cornwell *et al.* 1989). Wolszczan & Cordes (1987) have resolved the magnetosphere of a pulsar by using a related method involving measured fluxes rather than interferometric visibilities.

How is it possible to attain a resolution superior to what one would normally associate with a given telescope aperture? The answer lies in multi-path propagation which brings to each point on the observer plane many rays from an area of size $\approx r_{\mathrm{ref}}$ on the scattering screen. Effectively, therefore, there is already one stage of 'imaging' between the scattering screen and the ground, the aperture of this imaging instrument having a size $\approx r_{\mathrm{ref}}$. It is this first round of imaging that limits the resolution. The telescope on the ground is not the primary resolving agent, but is merely the device that collects the information.

The situation can be demystified a little further by noting that we can distinguish stars from planets by the simple fact that the former twinkle while the latter do not. From this difference we can tell that stars have angular sizes smaller than $\approx 1''$, and that planets are larger. How are we able to make this distinction when the eye by itself has much too small an aperture to resolve anything at the level of $1''$? It is the scattering in the Earth's atmosphere which enhances the ability of the eye, by providing an effective aperture of size $\approx r_{\mathrm{F}} \approx$ few cm. In fact, as mentioned earlier, a similar principle is used to measure angular diameters of extragalactic radio sources by using interplanetary scintillation. The situation with the snapshot image differs in important respects from these examples: (1) the snapshot image corresponds to strong not weak scattering, and therefore the effective aperture is r_{ref} not r_{F}, (2) it uses spatial information through image visibilities, not temporal information on the flux, and (3) it is more flexible and capable of real two-dimensional imaging. Nevertheless, the basic principle remains the same, namely that a 'telescope' in the sky enhances the capabilities of the instrument on the ground.

We are thus left with the following paradoxical situation. We normally think of scattering as something that degrades the ability of an imaging instrument, for

instance the seeing limit on ground-based optical telescopes imposed by the Earth's atmosphere. In weak scattering, using various techniques like speckle interferometry and self-calibration, we have learned to restore the full resolution of the telescope. The claim in the above papers is that, in the presence of strong scattering, we might be able to do even better than this. Using various techniques (yet to be developed in detail), we may actually be able to achieve a *higher* resolution than we could without the scattering!

References

Berry, M. V. & Upstill, C. 1980 Catastrophe optics: morphologies of caustics and their diffraction patterns. *Prog. Optics* **18**, 258–346.

Blandford, R. & Narayan, R. 1985 Low-frequency variability of pulsars. *Mon. Not. R. astr. Soc.* **213**, 591–611.

Blandford, R., Narayan, R. & Romani, R. W. 1986 Flicker of extragalactic radio sources and refractive interstellar scintillation. *Astrophys. J.* **301**, L53–L56.

Born, M. & Wolf, E. 1980 *Principles of optics: electromagnetic theory of propagation, interference and diffraction of light.* (808 pages.) New York: Pergamon Press.

Cohen, M. H., Gundermann, E. J. & Harris, D. E. 1967 New limits on the diameters of radio sources. *Astrophys. J.* **150**, 767–782.

Cole, T. W., Hesse, H. K. & Page, C. G. 1970 Long term variations of pulsar intensities. *Nature, Lond.* **225**, 712–713.

Coles, W. A., Frehlich, R. G., Rickett, B. G. & Codona, J. L. 1987 Refractive scintillation in the interstellar medium. *Astrophys. J.* **315**, 666–674.

Cordes, J. M., Rickett, B. J. & Backer, D. C. (eds) 1988 *Radio wave scattering in the interstellar medium.* (230 pages.) New York: American Institute Physics.

Cornwell, T. J. & Wilkinson, P. N. 1981 A new method for making maps with unstable radio interferometers. *Mon. Not. R. astr. Soc.* **196**, 1067–1086.

Cornwell, T. J., Anantharamaiah, K. R. & Narayan, R. 1989 The propagation of coherence in scattering – an experiment using interplanetary scintillation. *J. opt. Soc. Am.* A **6**, 977–986.

Dainty, J. C. 1984 Stellar speckle interferometry. In *Laser speckle and related phenomena* (ed. J. C. Dainty), pp. 255–320. (342 pages.) New York: Springer-Verlag.

Fiedler, R. L., Dennison, B., Johnston, K. J. & Hewish, A. 1987 Extreme scattering events caused by compact structures in the interstellar medium. *Nature, Lond.* **326**, 675–678.

Ghez, A. M. *et al.* 1991 Diffraction limited infrared images of the binary star T Tauri. *Astron. J.* **102**, 2066–2072.

Gochelashvily, K. S. & Shishov, V. I. 1975 Saturation of laser irradiance fluctuation beyond a turbulent layer. *Opt. quant. Electron.* **7**, 524–536.

Goodman, J. & Narayan, R. 1985 Slow pulsar scintillation and the spectrum of interstellar electron density fluctuations. *Mon. Not. R. astr. Soc.* **214**, 519–537.

Goodman, J. & Narayan, R. 1989 The shape of a scatter-broadened image. II. Interferometric visibilities. *Mon. Not. R. astr. Soc.* **238**, 995–1028.

Goodman, J., Romani, R. W., Blandford, R. D. & Narayan, R. 1987 The effects of caustics on scintillating radio sources. *Mon. Not. R. astr. Soc.* **229**, 73–102.

Gorham, P. W. *et al.* 1989 Diffraction-limited imaging. III. 30 mas closure phase imaging of six binary stars with the Hale 5 m telescope. *Astron. J.* **98**, 1783–1799.

Gwinn, C. R., Cordes, J. M., Bartel, N., Wolszczan, A. & Mutel, R. L. 1988 VLBI Observations of a pulsar's scattering disk. *Astrophys. J.* **334**, L13–L16.

Haniff, C. A., Mackay, C. D., Titterington, D. J., Sivia, D., Baldwin, J. E. & Warner, P. J. 1987 The first images from optical aperture synthesis. *Nature, Lond.* **328**, 694–696.

Hankins, T. H., Anantharamaiah, K. R., Blandford, R. D., Cornwell, T. J. & Narayan, R. 1989

Dynamic measurements of the solar-wind induced rotation measure and dispersion measure fluctuations at small solar radii. Proposal submitted to NASA June 1989.

Hewish, A., 1952 The diffraction of galactic radio waves as a method of investigating the irregular structure of the ionosphere. *Proc. R. Soc. Lond.* A **214**, 494–514.

Hewish, A. 1988 Radio observations of plasma irregularities in the solar wind. In *Radio wave scattering in the interstellar medium* (ed. J. M. Cordes, B. J. Rickett & D. C. Backer), pp. 82–86. (230 pages.) New York: American Institute Physics.

Hewish, A., Scott, P. F. & Wills, D. 1964 Interplanetary scintillation of small diameter radio sources. *Nature, Lond.* **203**, 1214–1217.

Hinder, R. A. & Ryle, M. 1971 Atmospheric limitations to the angular resolution of aperture synthesis radio telescopes. *Mon. Not. R. astr. Soc.* **154**, 229–253.

Jennison, R. C. 1958 A phase sensitive interferometer technique for the measurement of the Fourier transforms of spatial brightness distributions of small angular extent. *Mon. Not. R. astr. Soc.* **118**, 276–284.

Kaspi, V. M. & Stinebring, D. R. 1992 Long term pulsar flux monitoring and refractive interstellar scintillation. *Astrophys. J.* (In the press.)

Little, L. T. & Hewish, A. 1966 Interplanetary scintillation and its relation to the angular structure of radio sources. *Mon. Not. R. astr. Soc.* **134**, 221–237.

Matheson, D. N. & Little, L. T. 1971 Radio scintillations due to plasma irregularities with power law spectra: the interplanetary medium. *Planet. Space Sci.* **19**, 1615–1624.

Mutel, R. L. & Lestrade, J.-F. 1990 Interstellar scattering of the compact radio source $2005 + 403$. *Astrophys. J.* **349**, L47–L49.

Narayan, R. 1988 From scintillation observations to a model of the ISM – the inverse problem. In *Radio wave scattering in the interstellar medium* (ed. J. M. Cordes, B. J. Rickett & D. C. Backer), pp. 17–31. (230 pages.) New York: American Institute Physics.

Narayan, R. & Hubbard, W. B. 1988 Theory of anisotropic refractive scintillation: application to stellar occultations by Neptune. *Astrophys. J.* **325**, 503–518.

Narayan, R. & Goodman, J. 1989 The shape of a scatter-broadened image. I. Numerical simulations and physical principles. *Mon. Not. R. astr. Soc.* **238**, 963–994.

Narayan, R., Anantharamaiah, K. R. & Cornwell, T. J. 1989 Refractive radio scintillation in the solar wind. *Mon. Not. R. astr. Soc.* **241**, 403–413.

Narayan, R., Cornwell, T. J., Goodman, J. & Anantharamaiah, K. R. 1990 Radio scattering and imaging. In *Radio astronomical seeing* (ed. J. E. Baldwin & W. Shouguan), pp. 205–211. (275 pages.) New York: Pergamon Press.

Pearson, T. J. & Readhead, A. C. S. 1984 Image formation by self-calibration in radio astronomy. *A. Rev. Astr. Astrophys.* **22**, 97–130.

Prokhorov, A. M., Bunkin, F. V., Gochelashvily, K. S. & Shishov, V. I. 1975 Laser irradiance propagation in turbulent media. *Proc. IEEE* **63**, 790–811.

Ratcliffe, J. A. 1956 Some aspects of diffraction theory and their application to the ionosphere. *Rep. Prog. Phys.* **19**, 188–267.

Readhead, A. C. S. & Wilkinson, P. N. 1978 The mapping of compact radio sources from VLBI data. *Astrophys. J.* **223**, 25–36.

Readhead, A. C. S., Kemp, M. C. & Hewish, A. 1978 The spectrum of small-scale density fluctuations in the solar wind. *Mon. Not. R. astr. Soc.* **185**, 207–225.

Rickett, B. J. 1986 Refractive interstellar scintillation of radio sources. *Astrophys. J.* **307**, 564–574.

Rickett, B. J. 1990 Radio propagation through the turbulent interstellar plasma. *A. Rev. Astr. Astrophys.* **28**, 561–605.

Rickett, B. J., Coles, W. A. & Bourgois, G. 1984 Slow scintillation in the interstellar medium. *Astr. Astrophys.* **134**, 390–395.

Roddier, F. 1981 The effects of atmospheric turbulence in optical astronomy. *Prog. Optics* **19**, 281–376.

Romani, R. W., Blandford, R. D. & Cordes, J. M. 1987 Radio caustics from localized interstellar medium plasma structures. *Nature, Lond.* **328**, 324–326.

Romani, R. W., Narayan, R. & Blandford, R. D. 1986 Refractive effects in pulsar scintillation. *Mon. Not. R. astr. Soc.* **220**, 19–49.

Rumsey, V. H. 1975 Scintillations due to a concentrated layer with a power-law turbulence spectrum. *Radio Sci.* **10**, 107–114.

Scheuer, P. A. G. 1968 Amplitude variations in pulsed radio sources. *Nature, Lond.* **218**, 920–922.

Shapirovskaya, N. Y. 1978 Variability of extragalactic decimeter radio sources. *Soviet Astr.* **22**, 544–547.

Shishov, V. I. 1974 Effect of refraction on scintillation characteristics and average pulse shape of pulsars. *Soviet Astr.* **17**, 598–602.

Sieber, W. 1982 Causal relationship between pulsar long-term intensity variations and the interstellar medium. *Astr. Astrophys.* **113**, 311–313.

Smith, F. G. 1950 Origin of the fluctuations in the intensity of radio waves from galactic sources. *Nature, Lond.* **165**, 422–423.

Spoelstra, T. A. T. 1983 The influence of ionospheric refraction on radio astronomy interferometry. *Astr. Astrophys.* **120**, 313–321.

Tatarskii, V. I. & Zavorotnyi, V. U. 1980 Strong fluctuations in light propagation in a randomly inhomogeneous medium. *Prog. Optics* **18**, 207–256.

Thompson, A. R., Moran, J. M. & Swenson, G. W. 1986 *Interferometry and synthesis in radio astronomy*. (534 pages.) New York: Wiley.

Uscinski, B. J. 1977 *The elements of wave propagation in random media*. (153 pages.) New York: McGraw-Hill.

Uscinski, B. J. 1982 Intensity fluctuations in a multiple scattering medium. Solution of the fourth moment equation. *Proc. R. Soc. Lond.* A **380**, 137–169.

Wolszczan, A. & Cordes, J. M. 1987 Interstellar interferometry of the pulsar PSR 1237 + 25. *Astrophys. J.* **320**, L35–L39.